

# Nanostructure Engineering and Doping of Conjugated Carbon Nitride Semiconductors for Hydrogen Photosynthesis\*\*

Zhenzhen Lin and Xinchun Wang\*

Conjugated polymer semiconductors (CPSs) hold great promise in plastic electronics and optoelectronics because of their easy processability and their delocalized valence and conduction bands that favor charge transport.<sup>[1]</sup> In practice, CPSs are generally processed in the form of multi-junction thin films and coupled to chemical redox doping, for example, by oxidation to remove some delocalized electrons and by reduction to add electrons to an otherwise unfilled band, to create p-type<sup>[2]</sup> and n-type CPSs,<sup>[3]</sup> respectively. The functional CPSs have high electrical conductivity of around 0.1–10 kScm<sup>−1</sup> and have long been proposed for use as solar-energy transducers for artificial photosynthesis, however, thus far they have had limited success because traditional CPSs are unstable toward light irradiation in the presence of water and air.<sup>[4]</sup> They are also known to be restricted by the high binding energies of the Frenkel-type excitons that are quantum confined in 1D conjugated chains, while the low equilibrium/kinetic rigidity of 1D polymers accelerates the thermal-relaxation (recombination) processes of light-induced charge carriers.<sup>[5]</sup> It is therefore not surprising that the application of CPSs to wireless photochemical reactions is rarely covered, nowadays.

When expanding the dimension of CPSs from 1D to 2D, the exciton binding energies are in principle remarkably reduced, and thus, allow for fast charge transfer and separation;<sup>[6]</sup> however, stiff 2D CPSs are very rare and still challenge synthetic chemists and material designers.

Covalent carbon nitride (CN) chemistry offers a new way to study photochemistry, based on rigid 2D CPSs.<sup>[7]</sup> Graphite-like CN (g-CN) is built from poly(heptazine) heterocyclic planes packed together in a manner similar to graphite, with controllable band gaps and suitable band positions.<sup>[8]</sup> It is of particular interest that this 2D semiconductor is highly-stable and insoluble in most acids, bases, and solvents. g-CN has been shown to photocatalyze water splitting and organic photosynthesis,<sup>[9]</sup> even without optimization of the texture

and electronic structure. To modify g-CN, a variety of doping atoms have been incorporated,<sup>[10]</sup> along with texturing of g-CN in the forms of nanorods, hollow nanospheres, or mesozeolites.<sup>[11]</sup> Boron-modified (B-modified) g-CNs were reported for organosynthesis<sup>[10b]</sup> and bleaching dyes,<sup>[12]</sup> but when applied to photocatalytic water splitting they are virtually inactive.<sup>[10b]</sup> This is because the positive doping effects are often counteracted by the detrimental effects of the dopant residues, such as high trap-site densities and the spoiling of electronic structure when B-precursors and g-CN-precursors are chemically incompatible.<sup>[10b]</sup> The rational selection of precursors for both B atoms and g-CN is therefore crucial for developing robust polymeric semiconductors for water redox catalysis, preferably using inexpensive, earth-abundant, and largely available materials.

Motivated by intriguing graphene chemistry, the exfoliation of bulk g-CN to 2D atomic g-CN layers has been actively pursued to achieve the full potential of these materials, such as opening the energy gap of 2D atomic layers to transform graphene into semiconductors with promising opto-electronic properties.<sup>[13]</sup> However, the “top-down” fabrication of g-CN nanosheets is still in its infancy.<sup>[14]</sup> In our previous studies and others,<sup>[15]</sup> it was found that “bottom-up” polycondensation of CN-precursors, such as urea and trithiocyanuric acid, strongly altered the polymerization route because of the involvement of heteroatom groups as leaving motifs, creating some thin CN sheets in nanodomains. Herein, to strengthen this effect, sodium tetraphenylboron (Ph<sub>4</sub>BNa) was used as a dual-function modifier for the polycondensation of urea, because it contains phenyl leaving groups and B atoms that can modify g-CN nanosheets in situ to tune their surface chemistry by imparting acid sites on the surface of basic g-CN materials. Such Lewis acids are reactive surface centers that are also known to have additional value in photocatalysis by acting as exciton dissociation traps.<sup>[16]</sup>

B-modified g-CN samples were synthesized by a thermal-induced polymerization of urea and Ph<sub>4</sub>BNa in a one-pot fashion; both precursors are easily available, inexpensive, and sustainable. In brief, 10 g urea and a certain amount of Ph<sub>4</sub>BNa were dissolved in water with stirring, followed by heating at 80 °C to remove water until solid white mixture was produced. The mixture was then calcined at 550 °C to induce the co-condensation of the precursors. For simplicity, the resulting yellow samples were denoted as CNUB-*X*, where *X* is an arbitrary number that represents the amount of Ph<sub>4</sub>BNa added in the copolymerization (see Table 1). The texture, chemical structure, and surface morphology of the samples were characterized with various physical and chemical techniques. The performance of these B-containing CN nanosheet semiconductors was accessed in a H<sub>2</sub> photosyn-

[\*] Z. Lin, Prof. X. Wang  
Research Institute of Photocatalysis, Fujian Provincial Key Laboratory of Photocatalysis-State Key Laboratory Breeding Base, and College of Chemistry and Chemical Engineering, Fuzhou University Fuzhou 350002 (China)  
E-mail: xcwang@fzu.edu.cn

[\*\*] Supported by the National Basic Research Program of China (2013CB632405), the National Natural Science Foundation of China (21033003, 21173043), and the Department of Education of Fujian Province in China. The authors appreciate Prof. L. Li of Xiamen University (China) for the AFM measurements.

Supporting information for this article (experimental details) is available on the WWW under <http://dx.doi.org/10.1002/anie.201209017>.

**Table 1:** Physicochemical properties of g-CN and CNUB samples.

Catalyst	Ph <sub>4</sub> BNa <sup>[a]</sup> [mg]	SA <sup>[b]</sup> [m <sup>2</sup> g <sup>-1</sup> ]	PV <sup>[c]</sup> [cm <sup>3</sup> g <sup>-1</sup> ]	PD <sup>[d]</sup> [nm]	HER <sup>[e]</sup> [μmol h <sup>-1</sup> ]
g-CN	0	80	0.40	18.4	111
CNUB-1	3	133	0.64	17.5	166
CNUB-2	5	144	0.62	16.2	278
CNUB-3	10	131	0.70	21.1	208
CNUB-4	20	141	0.97	27.9	203

[a] The amount of Ph<sub>4</sub>BNa added in the co-polymerization; [b] the surface area; [c] pore volume; [d] average pore size determined by the BJH method; [e] H<sub>2</sub> evolution rate.

thesis assay, using cooperative Pt catalysts, electron donors, and visible-light illumination (greater than 420 nm).

First, we measured the XPS spectra of the modified samples to determine the incorporation of B atoms and their oxidation state in the CN framework. A clear B 1s XPS peak with a binding energy (BE) of 191.6 eV was observed for the CNUB-4 sample (Figure 1 a), corresponding to N-B-N coor-

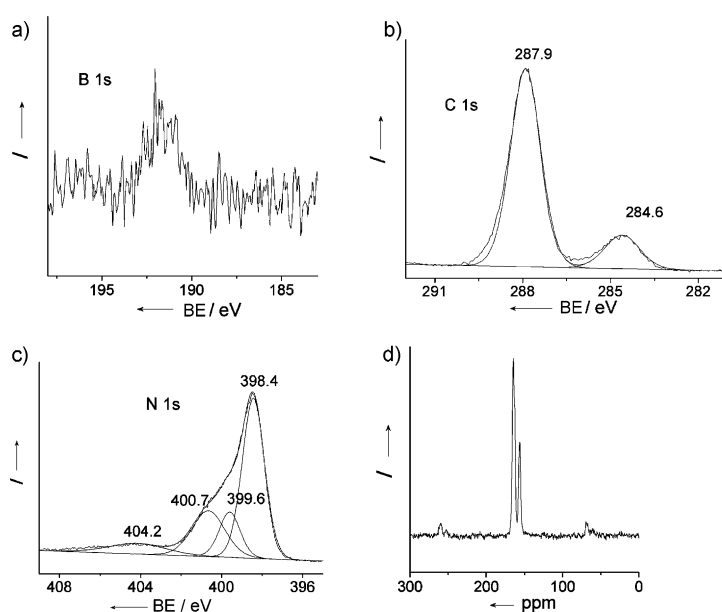


**Figure 1.** a–c) XPS and solid-state d) <sup>13</sup>C NMR spectra of CNUB-4.

dination.<sup>[12b]</sup> This indicates that some of the B atoms are introduced into the carbon sites of the CN matrix. To investigate the effect of B doping on the structure of the CN framework, the spectra of C 1s and N 1s were also analyzed (Figure 1 b and Figure 1 c, respectively). The C 1s signal shows mainly one carbon species with a BE of 287.9 eV, identified as an sp<sup>2</sup>-bonded carbon (C–C=N). The peak with BE of 284.6 eV was ascribed to carbon impurities.<sup>[15a]</sup> The N 1s XPS spectrum can be deconvoluted into four peaks with BEs at 398.4, 399.6, 400.7, and 404.2 eV. The strongest N 1s peak at 398.4 eV was assigned to sp<sup>2</sup>-bonded nitrogen in N-containing aromatic rings (C–N=C), whereas the weak peak at 399.6 eV is usually attributed to the tertiary nitrogen N–(C)<sub>3</sub> groups. The peak at 400.7 eV indicated the presence of amino groups

(C–N–H) and the peak at 404.2 eV was attributed to charging effects or positive charge localization in heterocycles.<sup>[15a]</sup> The carbon and nitrogen XPS analyses revealed that the chemical structure of g-CN is constructed from in-planar connection of tri-*s*-triazine subunits, as confirmed by the solid state <sup>13</sup>C NMR analysis (Figure 1 d). Because the intensity of the B peak is extremely weak compared to the others, the B-doped CN polymers were dominated by the heptazine structures. This suggests that the molecular structure of g-CN is mostly unaltered following modification with a small amount of B atoms, but it is enough to modify the semi-conductive properties, as in the well-known case of B-doped silicon.<sup>[17]</sup>

The structure and morphology of B-doped CNs were further examined by powder X-ray diffraction (XRD), Fourier transform infrared (FTIR), nitrogen sorption, transmission electron microscopy (TEM), and atomic force microscopy (AFM) measurements. The XRD diffractogram (Supporting Information, Figure S1) of the polymeric g-CN features two distinct reflections at 2θ = 13.0° and 27.5°, corresponding to an in-plane repeating motif and the stacking of the CN-conjugated layers along the (002) direction, respectively.<sup>[8]</sup> The XRD patterns of the CNUB materials are similar to that of the pristine CN polymer; however, the (002) diffraction of CNUB-4 (the heavily doped g-CN) is significantly weakened, which can be attributed to the disturbance of the graphitic structure by excessive B atoms (note: a B atom is bigger than C and N atoms). This is a strong indication of an alteration in the morphology of g-CN, for example, the delamination of the thick bulk g-CN to thin CN nanosheets of several atomic layers.

All FTIR spectra of as-obtained polymers show characteristic bands of aromatic CN heterocycles at 1200 to 1600 cm<sup>-1</sup> and tri-*s*-triazine units at 800 cm<sup>-1</sup> (Figure S2), similar to those of g-CN.<sup>[11]</sup> The vibrations of the B-related group (N–B–N) were hardly observed in the doped CN matrix, presumably due to the overlap of the band with that of the C–N vibrations.

The optical absorption spectra were used to investigate the effect of B modification on the electronic structure of g-CN. The obtained samples exhibited the typical absorption patterns of semi-conductors, shown in Figure 2. The band gaps of g-CN

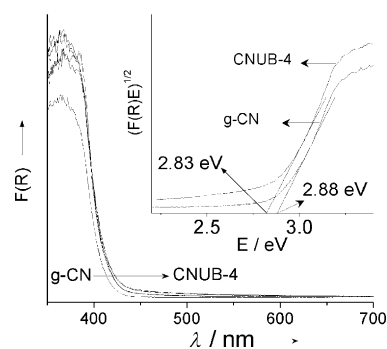


**Figure 2.** UV/Vis diffuse reflectance spectra of CNUB-X, with g-CN as reference and the corresponding Tauc plot (inset).

and the CNUB materials determined are 2.88 eV and 2.83 eV. On the other hand, the B-doped g-CN solids present a weak absorption tail, again reflecting the incorporation of B atoms into the g-CN frameworks. This modification, in principle, narrows the material gap and improves the ability of the material to harvest visible light.

Typical TEM images of pristine CN and CNUB are shown in Figure S3. Clearly, the pristine g-CN exhibits the typical layered platelet-like surface morphology (Figure S3) that changes to a thin, silk-like nanostructure after B doping (Figure S3 and Figure 3a), indicating the delamination effect. The thickness of the nanosheets is further confirmed by AFM analyses that revealed a thickness of approximately 2–5 nm for the B-doped g-CN sheets (Figure 3b and Figure S4).

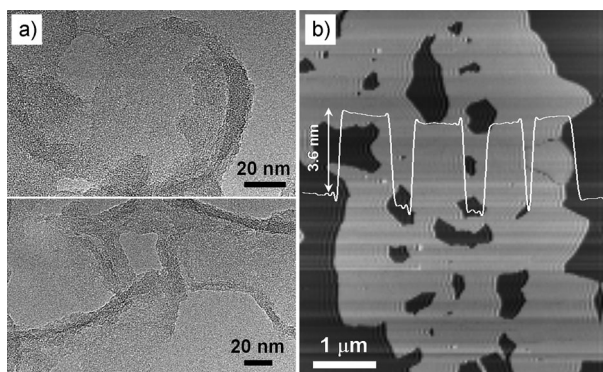


**Figure 3.** Typical a) TEM images, note: the top panel shows the curling of the CN layer, while the bottom panel shows a typical nanosheet; b) AFM images of CNUB. White line shows the height profile of CNUB from the AFM image.

These thin CN nanosheets are highly desirable for photochemical applications because the reduced thickness shortens the transport distance of charge from the bulk to the surface, whereby the photoredox reaction takes place. The delamination effect also induces the curling of CN layers in the nanodomains to lessen the surface tension (Figure 3a), somewhat similar to the formation of a carbon scroll by peeling graphite. On one hand, this enlarges the specific surface area of the B-doped samples and on the other hand, alters the electronic structure of CN by creating polar surface docking sites owing to the distortion of the  $\pi$ -conjugated orbital. The enlarged surface area (Table 1) not only facilitates mass transfer but also provides more active sites for surface-dependent reactions, which, together with the shorter charge-transport path and enhanced surface properties, are favorable for heterogeneous photocatalysis.

Photocatalytic hydrogen production by the samples loaded with 3 wt % Pt as a cocatalyst was evaluated under visible light irradiation ( $\lambda > 420$  nm).<sup>[4c]</sup> As shown in Figure 4a, the photocatalytic activity of all CNUB samples, in terms of hydrogen evolution rate (HER = 166, 278, 208, 203  $\mu\text{mol h}^{-1}$  for  $X=1, 2, 3$ , and 4, as shown in Table 1), were higher than that of the pure g-CN reference (HER =

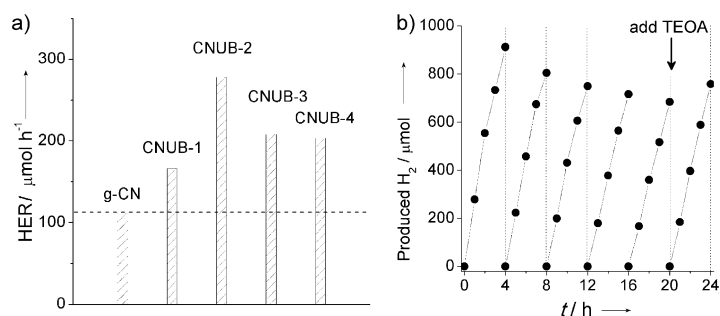


**Figure 4.** a) Hydrogen evolution rates (HER) of g-CN and CNUB-X photocatalysts. b) Stability test of H<sub>2</sub> photosynthesis (evacuation every 4 h) for a CNUB-2 sample under visible light irradiation ( $\lambda > 420$  nm). Note: 5 mL TEOA was added after the fifth run.

111  $\mu\text{mol h}^{-1}$ ). Undoubtedly, the CNUB polymers show a significant improvement in hydrogen evolution activity over the pristine one, which is presumably owing to the use of more visible light and the increased surface reactivity for the photocatalytic reaction. The additional boron functional groups on the surface might act as Lewis acid sites, which, together with the intrinsic Lewis base sites in carbon nitride polymers, create a metal-free organocatalyst containing both Lewis acid and Lewis base sites. This is somewhat similar to a frustrated Lewis pair.<sup>[18]</sup> Such acid and base centers in photocatalysts are of great interest and should, in principle, favor the fast splitting of light-generated excitons. Such Lewis pairs are also already known to facilitate the formation of hydrogen adatom centers on the acid-base sites and enhance the surface reactivity of the catalysts, and thus, promoting catalytic kinetics for (photo)chemical transformation.<sup>[19]</sup>

The stability of CNUB samples were also examined by operating the photocatalytic experiments under the same reaction conditions for several cycles (Figure 4b). A slight deactivation with time was noticed in the first five runs. When an appropriate amount of triethanolamine (TEOA) was added to the reaction solution, the activity of hydrogen evolution improved in the sixth run. Note that no obvious change in material structures was observed through XRD and FTIR examinations (Figures S5, S6) for the sample before and after reaction. This indicates that the decrease in the activity after the first run is mainly due to the decreased concentration of triethanolamine. Therefore, the (photo)-chemical stability of the conjugated CNUB as a nanosheet organocatalyst is acceptable for light-triggered hydrogen generation.

In summary, we have demonstrated the use of sodium tetraphenylboron as a multifunctional modifier of the self-polymerization of urea to control the texture, surface chemistry, and semiconductor properties of CN polymers in a simple one-pot fashion. The obtained B-modified CN nanosheets photocatalyze hydrogen evolution from a protic solution under visible light irradiation, and show a much higher activity than that of the pure urea-derived CN catalyst. The reduced layer thickness and the strengthened surface reactivity of g-CN maximize the material potential of 2D conjugated CN semiconductors. They are therefore promising as a new family of light-harvesting catalysts for the efficient

and sustained use of solar radiation for hydrogen photosynthesis, by junction with secondary semiconductors and coupling to the controlled deposition of a co-catalyst onto the two side surfaces.

Received: November 11, 2012  
Published online: January 7, 2013

**Keywords:** carbon nitride · conjugated polymers · doping · nanosheets · photosynthesis

- [1] a) A. Arias, J. MacKenzie, I. McCulloch, J. Rivnay, A. Salleo, *Chem. Rev.* **2010**, *110*, 3; b) A. Facchetti, *Chem. Mater.* **2011**, *23*, 733; c) H. Zhou, L. Yang, W. You, *Macromolecules* **2012**, *45*, 607; d) X. Zhu, C. Tian, S. Mahurin, S. Chai, C. Wang, S. Brown, G. Veith, H. Luo, H. Liu, S. Dai, *J. Am. Chem. Soc.* **2012**, *134*, 10478.
- [2] a) P. Ganesan, X. Yang, J. Loos, T. Savenije, R. Abellon, H. Zuilhof, E. Sudhölter, *J. Am. Chem. Soc.* **2005**, *127*, 14530; b) I. McCulloch, M. Heeney, C. Bailey, K. Genevicius, I. MacDonald, M. Shkunov, D. Sparrowe, S. Tierney, R. Wagner, W. Zhang, M. Chabiniy, R. Kline, M. McGehee, M. Toney, *Nat. Mater.* **2006**, *5*, 328; c) Q. Zheng, S. Chen, B. Zhang, L. Wang, C. Tang, H. Katz, *Org. Lett.* **2011**, *13*, 324.
- [3] a) D. Izuhara, T. Swager, *J. Am. Chem. Soc.* **2009**, *131*, 17724; b) H. Yan, Z. Chen, Y. Zheng, C. Newman, J. Quinn, F. Dötz, M. Kastler, A. Facchetti, *Nature* **2009**, *457*, 679; c) Y. Takeda, T. Andrew, J. Lobez, A. Mork, T. Swager, *Angew. Chem.* **2012**, *124*, 9176; *Angew. Chem. Int. Ed.* **2012**, *51*, 9042.
- [4] a) S. Allard, M. Forster, B. Souharce, H. Thiem, U. Scherf, *Angew. Chem.* **2008**, *120*, 4138; *Angew. Chem. Int. Ed.* **2008**, *47*, 4070; b) M. Schwab, M. Hamburger, X. Feng, J. Shu, H. Spiess, X. Wang, M. Antonietti, K. Müllen, *Chem. Commun.* **2010**, *46*, 8932; c) J. Zhang, M. Zhang, R. Sun, X. Wang, *Angew. Chem.* **2012**, *124*, 10292; *Angew. Chem. Int. Ed.* **2012**, *51*, 10145.
- [5] K. Hummer, P. Puschnig, S. Sagmeister, C. Draxl, *Mod. Phys. Lett. B* **2006**, *20*, 261.
- [6] a) P. Heremans, D. Cheyins, B. Rand, *Acc. Chem. Res.* **2009**, *42*, 1740; b) S. Jeong, D. Yoo, J. Jang, M. Kim, J. Cheon, *J. Am. Chem. Soc.* **2012**, *134*, 18233.
- [7] a) X. Wang, K. Maeda, A. Thomas, K. Takanabe, G. Xin, J. Carlsson, K. Domen, M. Antonietti, *Nat. Mater.* **2009**, *8*, 76; b) X. Wang, S. Blechert, M. Antonietti, *ACS Catal.* **2012**, *2*, 1596; c) X. Wang, K. Maeda, X. Chen, K. Takanabe, K. Domen, Y. Hou, X. Fu, M. Antonietti, *J. Am. Chem. Soc.* **2009**, *131*, 1680.
- [8] a) J. Zhang, G. Zhang, X. Chen, S. Lin, L. Möhlmann, G. Dołęga, G. Lipner, M. Antonietti, S. Blechert, X. Wang, *Angew. Chem.* **2012**, *124*, 3237; *Angew. Chem. Int. Ed.* **2012**, *51*, 3183; b) Y. Zhang, A. Thomas, M. Antonietti, X. Wang, *J. Am. Chem. Soc.* **2009**, *131*, 50; c) J. Zhang, X. Chen, K. Takanabe, K. Maeda, K. Domen, J. Epping, X. Fu, M. Antonietti, X. Wang, *Angew. Chem.* **2010**, *122*, 451; *Angew. Chem. Int. Ed.* **2010**, *49*, 441.
- [9] a) F. Su, S. Mathew, L. Möhlmann, M. Antonietti, X. Wang, S. Blechert, *Angew. Chem.* **2011**, *123*, 683; *Angew. Chem. Int. Ed.* **2011**, *50*, 657; b) F. Su, S. Mathew, G. Lipner, X. Fu, M. Antonietti, S. Blechert, X. Wang, *J. Am. Chem. Soc.* **2010**, *132*, 16299; c) X. Chen, J. Zhang, X. Fu, M. Antonietti, X. Wang, *J. Am. Chem. Soc.* **2009**, *131*, 11658.
- [10] a) Y. Zhang, T. Mori, J. Ye, M. Antonietti, *J. Am. Chem. Soc.* **2010**, *132*, 6294; b) Y. Wang, J. Zhang, X. Wang, M. Antonietti, H. Li, *Angew. Chem.* **2010**, *122*, 3428; *Angew. Chem. Int. Ed.* **2010**, *49*, 3356; c) G. Liu, P. Niu, C. Sun, S. Smith, Z. Chen, G. Lu, H. Cheng, *J. Am. Chem. Soc.* **2010**, *132*, 11642.
- [11] a) Y. Cui, Z. Ding, X. Fu, X. Wang, *Angew. Chem.* **2012**, *124*, 11984; *Angew. Chem. Int. Ed.* **2012**, *51*, 11814; b) J. Sun, J. Zhang, M. Zhang, M. Antonietti, X. Fu, X. Wang, *Nat. Commun.* **2012**, *3*, 1139; c) X. Chen, Y. Jun, K. Takanabe, K. Maeda, K. Domen, X. Fu, M. Antonietti, X. Wang, *Chem. Mater.* **2009**, *21*, 4093; d) E. Lee, Y. Jun, W. Hong, A. Thomas, M. Jin, *Angew. Chem.* **2010**, *122*, 9900; *Angew. Chem. Int. Ed.* **2010**, *49*, 9706.
- [12] a) S. Yan, Z. Li, Z. Zou, *Langmuir* **2010**, *26*, 3894; b) Y. Wang, H. Li, J. Yao, X. Wang, M. Antonietti, *Chem. Sci.* **2011**, *2*, 446.
- [13] a) K. Novoselov, A. Geim, S. Morozov, D. Jiang, Y. Zhang, S. Dubonos, I. Grigorieva, A. Firsov, *Science* **2004**, *306*, 666; b) M. Allen, V. Tung, R. Kaner, *Chem. Rev.* **2010**, *110*, 132; c) Z. Wu, A. Winter, L. Chen, Y. Sun, A. Turchanin, X. Feng, K. Müllen, *Adv. Mater.* **2012**, *24*, 5130.
- [14] P. Niu, L. Zhang, G. Liu, H. Cheng, *Adv. Funct. Mater.* **2012**, *22*, 4763.
- [15] a) J. Liu, T. Zhang, Z. Wang, G. Dawson, W. Chen, *J. Mater. Chem.* **2011**, *21*, 14398; b) G. Zhang, J. Zhang, M. Zhang, X. Wang, *J. Mater. Chem.* **2012**, *22*, 8083; c) J. Zhang, J. Sun, K. Maeda, K. Domen, P. Liu, M. Antonietti, X. Fu, X. Wang, *Energy Environ. Sci.* **2011**, *4*, 675.
- [16] X. Wang, J. Yu, Y. Hou, X. Fu, *Adv. Mater.* **2005**, *17*, 99.
- [17] a) E. Bustarret, C. Marcenat, P. Achatz, J. Kačmarčík, F. Lévy, A. Huxley, L. Ortéga, E. Bourgeois, X. Blase, D. Débarre, J. Boulmer, *Nature* **2006**, *444*, 465; b) N. Fukata, *Adv. Mater.* **2009**, *21*, 2829; c) R. Liu, G. Yuan, C. Joe, T. Lightburn, K. Tan, D. Wang, *Angew. Chem.* **2012**, *124*, 6813; *Angew. Chem. Int. Ed.* **2012**, *51*, 6709.
- [18] D. Stephan, *Org. Biomol. Chem.* **2008**, *6*, 1535.
- [19] a) D. Stephan, G. Erker, *Angew. Chem.* **2010**, *122*, 50; *Angew. Chem. Int. Ed.* **2010**, *49*, 46; b) S. Podiyanchari, R. Frohlich, C. Daniliuc, J. Petersen, C. Muck-Lichtenfeld, G. Kehr, G. Erker, *Angew. Chem.* **2012**, *124*, 8960; *Angew. Chem. Int. Ed.* **2012**, *51*, 8830; c) L. Greb, P. Ona-Burgos, B. Schirmer, S. Grimme, D. Stephan, J. Paradies, *Angew. Chem.* **2012**, *124*, 10311; *Angew. Chem. Int. Ed.* **2012**, *51*, 10164.